JACS
JOURNAL OF THE AMERICAN CHEMICAL SOCIETY

ARTICLE

pubs.acs.org/JACS

Direct Control of Electron Transfer to the Surface-CO Bond on a Pt/TiO_2 Catalytic Diode

Prashant Deshlahra,[†] William F. Schneider,[†,‡] Gary H. Bernstein,[§] and Eduardo E. Wolf[*,†]

Departments of [†]Chemical and Biomolecular Engineering, [‡]Chemistry and Biochemistry, [§]Electrical Engineering, University of Notre Dame, Notre Dame, Indiana 46556, United States

Supporting Information

ABSTRACT: We study CO adsorption on a multilayer catalytic diode in which electron transfer at the metal−semiconductor (Pt/TiO_2) junction is controlled by an applied external voltage. The multilayer diode structure enhances infrared absorption signals from CO molecules adsorbed on the small area Pt surface. We find that the diode behaves like a Schottky junction and that changes in electron transfer at the junction are directly correlated with reversible shifts in the vibrational frequency of adsorbed CO. Infrared polarization and incidence angle dependent studies show that the magnitude of vibrational frequency shift varies with orientation of the molecules being probed and increases with proximity to the Pt/TiO_2 interface. The results demonstrate the ability to control the metal−adsorbate bond through external electronic modifications of a metal−support junction. The catalytic diode can potentially provide control of the surface chemical bond by an external voltage, providing a new approach for investigations in heterogeneous catalysis, sensors, and plasmonic devices.

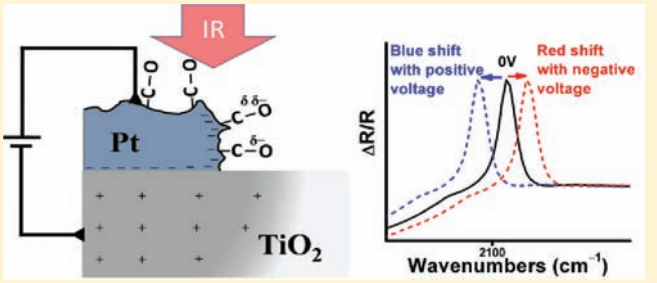

1. INTRODUCTION

Heterogeneous supported catalysts are complex materials with their activity and selectivity determined by a number of parameters such as composition, shape and size of crystallites, nature of the support, and in general by surface properties, which often change in response to the reaction environment.[1,2] Model catalysts allow study of these parameters by introducing the complexity of real catalytic materials in a controlled way.[3−8] Nanofabrication techniques can, in principle, be used to prepare catalysts with a precise control over structure and composition, and are thus potentially useful in catalysis research. One of the early attempts in this direction was made in our laboratory about 15 years ago. A regular array of Pt particles on a flat silica support was prepared using optical lithography, and its activity for butadiene hydrogenation reactions was studied.[9,10] While not explicitly stated in these papers, the concept of controlling the surface electron density on Pt particles by a bias voltage, as in a catalytic diode, a term introduced more recently by Somorjai and co-workers,[11,12] was explored and reported in a related patent.[13] Unfortunately, the microfabrication techniques available to us at that time were not suitable for fabricating nanostructures, and no special effect of a bias external voltage was detected. In recent years, Somorjai and co-workers have explored several modern nanolithography techniques to fabricate similar structures at the nanoscale[14] and prepared a catalytic nanodiode.[11,12] Following early reports from Nienhaus and co-workers,[15,16] they used the catalytic diode to measure continuously generated hot-electrons as a result of the energy released from the catalytic oxidation of CO.

The aim of our work is to prepare new versions of these nanocatalysts for studying electronic effects associated with metal−support junctions. Electronic effects have been known in catalysts for over 50 years, since the work of Schwab[17,18] and Solymosi,[19] and are often invoked to explain catalytic effects involving electron transfer between support and the metal catalyst. Early explanations of these effects were based on bulk junction diagrams which predicted that such transfer would occur between a semiconductor support and a metal surface. These effects are sometimes referred as electronic effects due to strong metal support interactions.[20,21] No *direct* verification that controlling such electron transfer can modify a metal−adsorbate bond has been obtained since these concepts were proposed, although many indirect measurements have been conducted for metal catalyst on reducible oxide supports, implying that such effects exist.[22−30] Early theoretical works on electron transfer from a support to a metal were inconclusive,[31] and the subject has been a matter of intense debate in the literature.[32,33]

In recent years, electronic effects have been examined in molecular adsorbates, metal ad-atoms or small clusters on ultrathin well-ordered oxide films deposited on a single-crystal metal substrate.[34−38] Initial model predictions were later used to rationalize experimentally observed adatom ordering, cluster arrangements, and changes in reactivity on ultrathin oxides.[39−42] Tunable catalysts with properties changing as a function of oxide

Received: March 25, 2011
Published: September 26, 2011

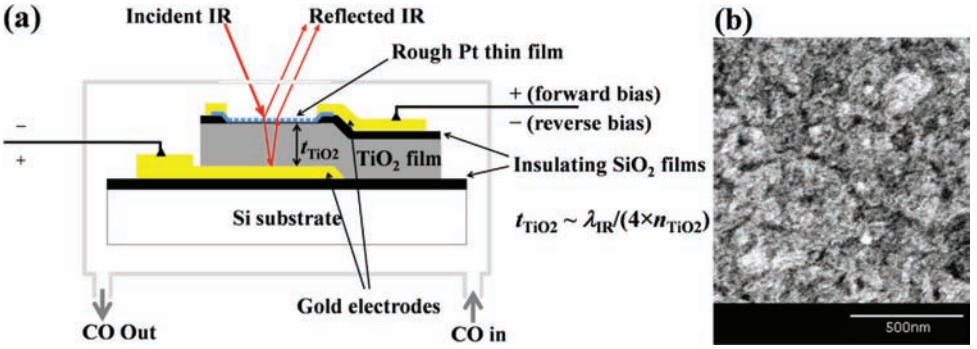

Figure 1. (a) Schematic of a catalytic diode with $Pt/TiO_2/Au$ multilayer structure. (b) SEM image showing the rough Pt thin film of a catalytic diode.

thickness have been proposed based on these results.[43] In these systems, electron transfer occurs by direct tunneling from metal substrate to adatom through an insulating oxide[34] or metal substrate induced modification of electron exchange between molecular adsorbate and immediate one or two layers of oxide surface atoms,[36] as well as structural effect of the relaxation of ultrathin films.[8]

In contrast to the results on ultrathin oxides, in more conventional metal catalysts on reducible oxides, electron transfer can occur between the metal particle and the bulk of the adjacent oxide support. A simple calculation based on energy band diagrams[44,45] of such systems predicts that the charge depletion region can extend at least up to several nanometers into a semiconductor oxide, such as titania. The results reported here relate to the latter phenomena and are relevant to industrial catalysts in which reaction rates are affected by the nature of the support. The study of electronic effects in metal−oxide systems has been limited by the lack of experimental capability to *directly* induce and observe the effect of electron transfer on adsorbates without modifying the structure and composition of the supported catalysts. In this work, we demonstrate such effects in a catalytic diode that introduces an external bias voltage as a new variable to induce electron transfer in much the same way as it is used in electronic devices.

We performed a density functional theory (DFT) study of CO adsorption on a Pt(111) surface subjected to modification of surface electronic states by an external electric field. The results and analyses showed shifting of the vibrational frequency of CO, known as the vibrational Stark effect,[46] and corresponding field induced changes in its equilibrium adsorption geometry and adsorbate electron densities.[47] While infrared frequency shifts of adsorbates on metal surfaces doped with alkali ions are well-known[48,49] in these systems, such electronic effects cannot be decoupled from local changes in surface concentrations induced by the alkali ions. Frequency shifts due to electric field have been observed on electrochemical electrode surfaces[46,50] and single crystal surfaces with external field imposed under ultrahigh vacuum (UHV),[51] but **not** on metal−support junction of supported catalysts in the presence of adsorbates. The main limitation on supported catalysts is the lack of electrical continuity among the metal crystallites dispersed on the support that does not allow controlling electric fields at the metal−support junctions. A catalytic diode provides the continuity in the junction that can be connected to an external voltage. For detection of such effects near these metal−support junctions however, a technique capable of sensing infrared absorption signals from CO adsorbed on small-area Pt films and nanostructures was needed. This was achieved by developing a new multilayer enhanced infrared reflection absorption spectroscopy (MEIRAS) technique in our laboratory.[52,53] The multilayer structure was realized by adding a bottom reflecting gold film below the metal−semiconductor junction formed by the top catalytic metal thin film and the intermediate oxide (TiO_2) film. We found that metal−oxide−metal multilayer structures introduced in the catalytic diode create optical interference effects that significantly enhance the FTIR sensitivity at the optimum oxide layer thickness. This enhancement allows atmospheric-pressure CO adsorption studies without the need of special instrumentation such as polarization-modulation infrared reflection absorption spectroscopy (PM-IRAS)[54,55] and sum frequency generation spectroscopy (SFG).[56] A MEIRAS study on nanofabricated Pt nanowire catalysts on TiO_2 support showed a significant gradual shift toward lower wavenumbers, in the peak position of adsorbed CO, with decrease in nanowire width, due to an increase in Pt/TiO_2 exposed interfaces per unit Pt area.[52,53] We performed further theoretical analysis of the interference effects to fully understand the sensitivity enhancement mechanism, and interpret the spectra obtained using this new technique.[57] The analysis showed that at small incidence angles the sensitivity to vibrational modes with dipole projections tangential to the surface is significantly greater than the sensitivity to projections normal to the surface. The relative sensitivity between tangential and normal modes can however be tuned by changing incidence angle of the parallel polarized radiation. This property can be used to probe the orientation of molecules by varying the angle of incidence of a polarized infrared beam incident on the catalytic diode as experimentally demonstrated for the first time in this work.

In this work, using the MEIRAS technique, we study the effect of applying an external voltage to a catalytic diode on the CO molecules adsorbed near the Pt/TiO_2 junctions. The voltage induced electronic modification leads to a reversible shift in the vibrational frequency of CO, demonstrating directly for the first time the effect of controlling electron transfer at metal−support junction on an adsorbed molecule. Fitting of spectral band areas to band center shifts and incidence angle dependent MEIRAS experiments show that, unlike uniform single crystal surfaces, the effect of electron transfer is dependent on the local geometry of the diode and the orientation of adsorbates being probed.

2. EXPERIMENTAL METHODS

Catalytic diodes prepared for this study consist of a Pt/TiO_2 junction with an active area of 9 mm^2 connected to a bottom and a top gold electrode (Figure 1a). Each layer of the diode was patterned using optical lithography and the metal films were deposited using electron beam evaporation followed by a liftoff process. These processes were carried out in a particle free class-100 clean-room environment to minimize the defects such as pin-holes in the deposited layers. First, a bottom gold electrode layer with Ti/Pt/Au film of 10 nm/15 nm/40 nm thicknesses was deposited on a silicon (100) wafer with a 100 nm insulating thermal oxide. A 250 nm Ti film was deposited covering half of the bottom gold electrode followed by thermal oxidation in dry air at 525 °C for 24 h. The oxidation process yielded about 550 nm thick TiO_2 film. Next, a 50 nm SiO_2 layer covering the whole wafer was deposited using plasma enhanced chemical vapor deposition (PECVD). This insulating SiO_2 layer was removed from the active area of the diode and the bottom gold pad by etching in a 10% buffered hydrofluoric (HF) solution for 10 s. After etching, an ultrathin SiO_2 layer of approximately 4 nm thickness, as estimated from PECVD deposition time, was redeposited on the active area. This was followed by deposition of a 5 nm Pt film and the top gold electrode consisting of a 10 nm/90 nm thick Pt/Au film. The 5 nm Pt film made a rectifying junction with the TiO_2 and the ultrathin SiO_2 acted as a tunnel barrier that improved the rectifying behavior of the Schottky junction and slightly modified the junction barrier height.[58]

The bottom reflecting gold electrode, the TiO_2 film, and the top Pt film were designed to form an optimum multilayer structure. The thickness of TiO_2 (t_{TiO_2}) is approximately a quarter of the wavelength of infrared (λ_{IR}) corresponding to C−O stretching vibrational mode (2100 cm^{-1}) divided by the refractive index of TiO_2 (n_{TiO_2}):

$$t_{TiO_2} \sim \frac{\lambda_{IR}}{4 \times n_{TiO_2}} \quad (1)$$

This quarter-wave matching created optimum interference conditions for the MEIRAS study of CO adsorption on a Pt surface.[52,57] The thermal oxidation of vapor-deposited Ti led to a rough TiO_2 film. As a result, the 5-nm Pt film deposited on the top of TiO_2, although electrically continuous, had a discontinuous, cracked surface (Figure 1b) with exposed Pt/TiO_2 interfaces available for CO adsorption. Thus, the multilayer structure involving a thin Pt film itself constituted a diode without the need of nanostructures or nanowires with exposed edges as originally designed.

MEIRAS experiments were performed using a Bruker Equinox 55 spectrometer and an optical assembly to reflect the infrared beam from the catalytic diode sample (Harrick, Praying Mantis). In experiments with constant angle of incidence, an angle of about 20° from the surface normal was used for measurement of the wavelength dependent reflectance of the sample and the CO adsorption MEIRAS experiments on catalytic diodes. The catalytic diode sample was placed in an *in situ* stainless steel infrared reaction cell (Harrick, HVC-DRP4) modified, as described elsewhere,[52,53] for performing MEIRAS measurements and introducing electrical contacts to bias the sample. The gas flow rates and temperature were controlled by mass flow and temperature controllers, respectively. The temperatures reported here are measured by a thermocouple touching the sample stage slightly away from sample surface and were higher than actual sample surface temperatures. A source-measure unit (Keithley 2400) was used for applying an external voltage and measuring the current through the device. After placing the sample in the reaction cell, a background infrared measurement was taken at 75 °C with helium flowing in the cell. The Pt surface of the diode was reduced in 5% CO in helium for 30 min at 175 °C, then cooled down to 75 °C. MEIRAS measurements were taken with and without an external bias voltage, after allowing the sample to equilibrate at 75 °C for 30 min with 1% CO (corresponding to ~8 Torr CO partial pressure) continuously flowing in the reaction chamber during the experiment. This process kept the Pt surface completely saturated with adsorbed CO molecules. The spectra were collected using a DTGS detector by taking 128 scans with a resolution of 8 cm^{-1}, which took about 4 min for each measurement. In addition, in selected experiments, measurements were conducted by introducing a ZnSe wire-grid polarizer (New Era Enterprises) in the path of the incident infrared beam, along with the use of a variable angle reflection accessory (Seagull, Harrick Scientific). These measurements were performed using a MCT detector at a resolution of 4 cm^{-1} in about 2 min for 256 scans.

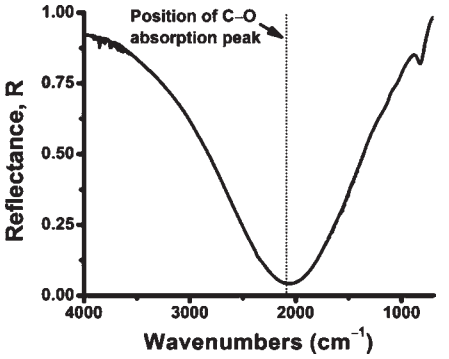

Figure 2. Reflectance of the $Pt/TiO_2/Au$ multilayer structure of the catalytic diode sample as a function of the incident infrared wavenumber.

3. RESULTS AND DISCUSSION

3.1. Optical and Electrical Characterization of Multilayer Catalytic Diode. Figure 2 shows reflectance of the multilayer catalytic diode sample relative to a 100 nm reflecting gold film used as a reference. Unlike the reflecting metal film, which has a reflectance close to 1 for all mid-infrared wavelengths, the reflectance of multilayer structure is strongly dependent on wavelength. The sample has minimum reflectance near the wavenumber of the absorption band of C−O stretching mode vibrations as the TiO_2 layer was designed to match the quarter-wave condition described by eq 1. This optical behavior of the multilayer structure is in agreement with previous work performed in our laboratory for MEIRAS using $Pt/SiO_2/Au$ multilayer catalysts.[52] Decreased reflectance of the sample along with increased surface intensity of the incident radiation, due to favorable optical interference, leads to overall signal enhancement as well as sensitivity to vibrational modes with projections tangential to the multilayer surface.[57] To test the effect of external voltage applied to the catalytic diode on optical properties of multilayer structure without any CO molecules adsorbed, we measure the wavelength dependent reflectance with external voltages varying up to ±2 V. The reflectance of the sample remains identical to the 0 V reflectance shown in Figure 2 (see Supporting Information), which confirms that the external voltage induced shifts in vibrational frequency of CO adsorbed on the catalytic diode during the experiment is not an artifact of changes in the optical response of the multilayer structure. The Pt/TiO_2 metal-semiconductor Schottky junction is characterized by measuring the current density (J = current/diode active area) versus voltage ($J-V$) of the catalytic diode. A rectifying $J-V$ behavior confirmed a Schottky junction with barrier height of about 1.2 V. Similar $J-V$ measurements performed on test devices without a Pt/TiO_2 active area, having a continuous layer

dx.doi.org/10.1021/ja2020789 |J. Am. Chem. Soc. 2011, 133, 16459–16467

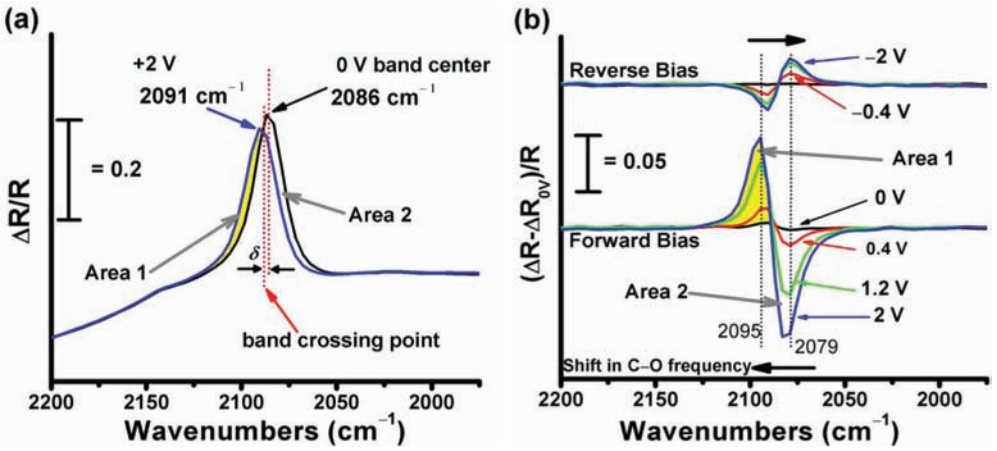

Figure 3. (a) Comparison of full MEIRAS vibrational spectra of CO adsorbed on the Pt surface of the catalytic diode with no biasing and an external bias of 2 V. (b) Difference spectra showing the shifts in CO vibrational modes as a result of applied bias voltage. The shift in MEIRAS peak position results in a positive (Area 1) and a negative (Area 2) peak in the difference between the biased and unbiased spectra.

of insulating SiO_2 between Pt and TiO_2, shows an insulating behavior (see Supporting Information). This comparison confirmed that the electron transport channel in the working catalytic diode is through the Pt/TiO_2 junction in the active area of the device.

3.2. Effect of Bias Induced Electron Transfer. Figure 3a shows the MEIRAS spectrum of CO adsorbed on the catalytic diode sample with and without external voltage. The spectra are shown as a normalized change in the reflectance of the sample due to infrared absorption by the adsorbed CO as a function of wavenumber:

$$\frac{\Delta R}{R} = \frac{R - R_0}{R_0} \tag{2}$$

Where, R_0 and R are the reflectance of bare substrate and reflectance after adsorption of CO, respectively. An infrared absorption spectrum generally appears as negative peaks when reflectance units are used. The catalytic diode samples used in this work, however, show inverted peaks that are positive in reflectance spectra, due to optical effects analyzed in previous work in our laboratory[57] as well as observed elsewhere.[59,60] The inverted peak shape was retained on this sample as the peak decreased in size during slow desorption of adsorbed CO and no positive and negative, derivative-like peaks were observed. This showed that the inverted peak shape occurring due to multilayer structure of the sample does not change with surface CO coverage.

When an external bias of 2 V is applied to the diode, the CO absorption band reversibly shifts to higher wavenumbers. This shift due to biasing is shown in Figure 3b as the difference spectra relative to the spectrum on the unbiased sample, defined as,

$$\left(\frac{\Delta R}{R}\right)_V - \left(\frac{\Delta R}{R}\right)_{V=0} \tag{3}$$

The difference spectrum appears as a positive peak (Area 1 in Figure 3) at the new shifted wavenumber and a negative peak (Area 2) at the original wavenumber, indicating the direction of C−O vibrational frequency shift with external voltage. The crossing point of the original 0 V MEIRAS band and the shifted band appears as zero crossing point between negative and

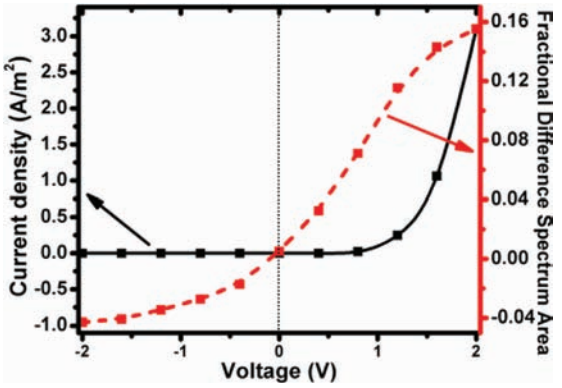

Figure 4. Measured *in situ* $J-V$ behavior of a catalytic diode and fractional area of the difference spectra (F_{diff}) versus external bias voltage.

positive peaks of the difference spectra. The position of positive and negative peaks differs by 12−16 cm^{-1} in the measured spectra. The magnitude of the shift increases gradually with bias voltage, as shown by the increase in the areas under of the difference spectra. On reverse biasing, that is, when a negative voltage is applied to the diode, the vibrational frequency shifts to lower wavenumbers (red shift). On forward biasing, the shift is toward higher wavenumbers (blue shift) and the magnitude of the difference spectrum area is larger than that at the same voltage applied in reverse bias. The band shift is reversible, returning to initial position on removing the external bias. The 0 V band shape and position remained unchanged before, during, and after the experiment, confirming that the CO coverage does not change during the experiment.

Figure 4 shows the electric current density (J) through the device and the fractional difference spectrum areas measured on a CO-covered Pt surface versus applied voltages ranging from −2 to 2 V. The reported current densities are the average of the measurements over 4 min durations collected in real time during the measurement of MEIRAS spectra in the presence of external bias voltage. The current density is very small for reverse bias and small forward bias, but shows a steep rise beyond 1 V and reaches 3 A m^{-2} at 2 V. This rectifying $J-V$

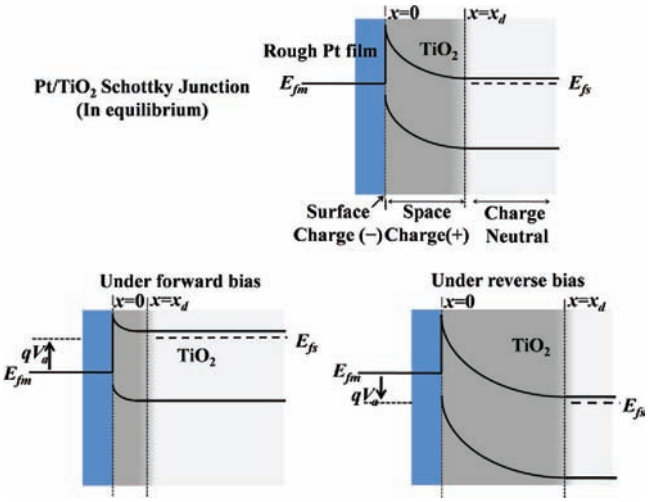

Figure 5. Band diagrams showing the effect of external voltage on a Pt/TiO_2 Schottky junction.

behavior confirms a metal−semiconductor Schottky junction at the Pt/TiO_2 interface of catalytic diode. The magnitude of shift in CO vibrational frequency as a function of external voltage can be quantified in terms of the fractional difference spectra area, F_{diff}, defined as the area under the difference spectrum A_{diff} as a fraction of the total MEIRAS peak area A_{total} at no external bias:

$$F_{diff} = \frac{A_{diff}}{A_{total}} \quad (4)$$

The difference spectrum area A_{diff} is calculated here as the average of the areas under positive and negative peak seen in Figure 3b. The positive value of F_{diff} on forward biasing corresponds to a peak shift to higher wavenumbers, whereas negative peak areas on reverse biasing imply a shift to lower wavenumbers with respect to the 0 V MEIRAS peak. The magnitudes of F_{diff} are larger for forward bias, reaching 15% at +2 V compared to 4% at −2 V. This difference in magnitude of shifts for forward and reverse bias can be explained in terms of the electronic properties of Pt/TiO_2 junctions.

A Pt/TiO_2 Schottky junction is formed by transfer of electrons from TiO_2 to Pt due to difference in electronic energy levels in the two materials. This electron transfer leads to the formation of a positively charged depletion region (space charge region) inside the TiO_2 and a negative electric field on the Pt surface, which should be experienced by the adsorbates that are close to the junction. Figure 5 shows typical schematic band diagrams of metal−semiconductor interfaces including the effect of the applied voltage (V_a) in shifting the relative Fermi levels of the metal (E_{fm}) and semiconductor (E_{fs}), as well as the spreading or narrowing of the space charge region in the semiconductor with a corresponding transfer of electrons to or from the metal at the junction. Within the full depletion approximation, the change in this interfacial electric field E at an ideal planar Schottky junction with an external applied voltage V_a is given by:[44]

$$E_{x=0} = \frac{qN_d x_d}{\varepsilon_s} \quad (5)$$

where, x is the distance away from the Pt/TiO_2 interface into the TiO_2 region as shown in Figure 5, q is the electronic charge, N_d is the carrier density in TiO_2, ε_s is the permittivity of TiO_2, and x_d is the width of the depletion region which changes with applied voltage as:

$$x_d = \sqrt{\frac{2\varepsilon_s}{qN_d}(\phi_i - V_a)} \quad (6)$$

Where, ϕ_i is the built-in potential of Pt/TiO_2 junction and V_a is the applied external voltage.

Figure 6a shows this trend of change in the junction electric field with external voltage for a built-in potential of 1.2 V. The change in electric field is higher under forward bias, which causes a larger change in difference spectrum area observed in Figure 4. Figure 6b shows the measured difference spectrum area as a function of the electric field estimated from Figure 6a and indicates that the trends for forward and reverse bias are similar. There was no direct correlation between the difference spectrum area and the current through the junction (Figure 4), confirming that it is the electric field due to charge accumulation at the junction and not the current flow that causes the peak shift. A further confirmation was obtained by conducting these experiments on samples that did not show a rectifying ($J-V$) behavior. No shift in peak position was observed on these samples, even at large applied voltages.

A red shift in C−O stretching frequency under reverse bias due to a more negative junction electric field indicates weakening of C−O bonds and implies a stronger Pt−C bond in the adsorbed molecule. Thus, biasing can in principle be used to modify the chemisorbed state of molecules on supported catalysts in a catalytic diode. The effect is opposite for forward biasing that caused a blue shift in C−O stretching frequency. The trends are consistent with DFT calculations of CO on Pt(111) surfaces under uniform electric field which predict a red shift on applying a negative field and vise versa.[47] The DFT based analyses also showed that a red shift in vibrational frequency corresponds to increased electron density in the $2\pi^*$ states of CO molecules, consistent with the mechanism of electron transport in the catalytic diode. These calculations predicted a shift of 45 cm^{-1} in the presence of a 1 V/Å external electric field. The actual magnitude of electric field built-up at the exposed Pt/TiO_2 junctions in the present study is unknown, but the magnitude of shifts is smaller than the DFT predictions at 1 V/Å. The magnitude of shift in the peak with applied voltage will depend on several factors, including Pt film continuity, exposed Pt/TiO_2 interface available for CO adsorption, the role of SiO_2 tunneling barrier, and the charge carrier density in TiO_2, which determines the junction electric field strength. A detailed study of these parameters and MEIRAS experiments involving different incidence angles and polarized radiation can lead to improved understanding of the extent to which an interfacial electric field affects the adsorbates in supported catalysts. The morphology of a cracked Pt film represents interconnected particles with lesser fraction of exposed interfaces than well-separated supported metal particles, but gives the unique advantage of using an external voltage to induce electron transfer. The effect of these geometric parameters can in principle be explored by nanolithographic patterning of Pt film, which can provide control over the fraction of interfaces.

3.3. Analysis of Nonuniformity of Vibrational Frequency Shifts. Unlike a flat single crystal surface subjected to a uniform

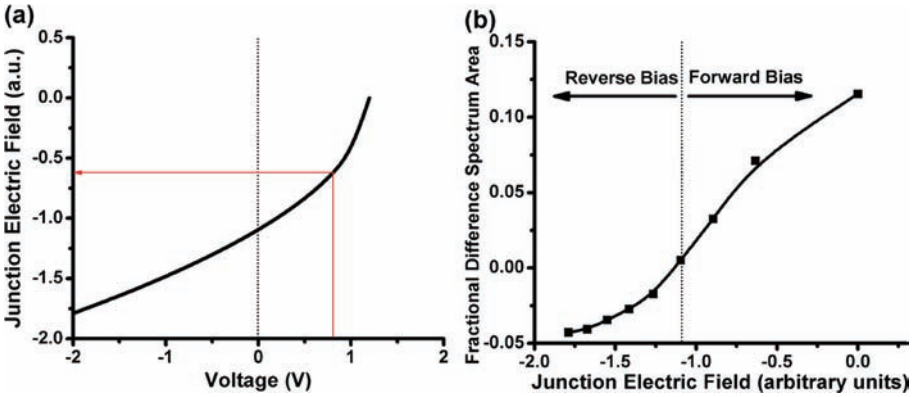

Figure 6. (a) Trends in electric field (in arbitrary units) at the Pt/TiO_2 interface estimated from an ideal Schottky junction model [eq 4]. (b) Relation between the measured difference spectrum peak area and the junction electric field from (a).

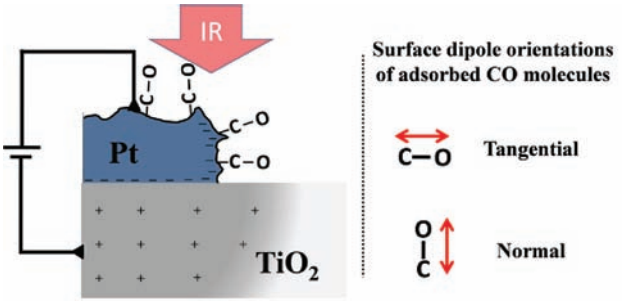

Figure 7. Schematic representation of local geometry and charge distribution of catalytic diode near the Pt/TiO_2 interfaces exposed to CO molecules.

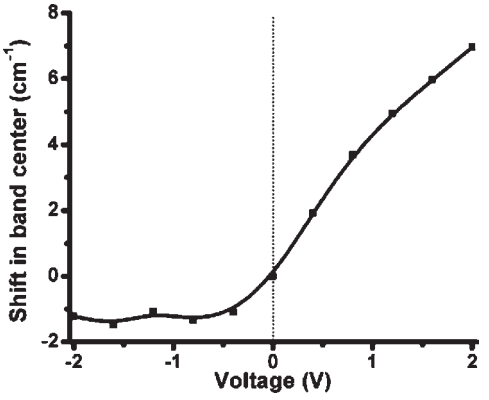

Figure 8. Average band center shifts of MEIRAS spectrum of CO as a function of external voltage.

electric field (i.e., the vibrational the Stark effect), the CO molecules adsorbed on a catalytic diode are expected to experience a nonuniform frequency shift depending on the proximity to the Pt/TiO_2 interface as schematically illustrated in Figure 7. To estimate the extent of nonuniformity in the shift, we estimate the band center shifts and difference spectrum areas for an ideal uniform shift, and compare it with the experimental difference spectrum areas. If the entire ensemble of CO molecules comprising the MEIRAS band experienced a uniform shift of 2δ, the band center will shift with virtually no change in its shape. In this case, the crossing point of the original and shifted bands (Figure 3a) will be δ away from original band center. Thus, the position of zero-crossing point of the difference spectra (Figure 3b) obtained at different voltages can be used to approximately estimate the band center shift 2δ. This average shift in band center, shown in Figure 8, has a form similar to the change in fractional difference spectrum area F_{diff} (Figure 4) with the forward bias shift being larger than the reverse bias shift. The fractional difference spectrum area F^{L}_{diff}, of a uniformly shifting Lorentzian band can then be calculated as a function of the band center shift 2δ using the following relation (see Supporting Information for derivation):

$$F^{L}_{diff} = \frac{A^{L}_{diff}}{A} = 2\tan^{-1}\left(\frac{2\delta}{w}\right) \quad (7)$$

where, A^{L}_{diff}, A, and w are the difference spectrum area, full peak area, and width of a band of the form of a Lorentzian function, respectively. If the entire ensemble of CO molecules experienced a uniform shift of 2δ, the difference peak area will change as F^{L}_{diff} described by eq 7. However, the measured F_{diff} values on the catalytic diode are smaller than this estimated value, and the fraction of CO molecules being probed, that exhibit an average shift of 2δ, can be estimated as the ratio of F_{diff} and F^{L}_{diff} shown in Table 1. Although not intended to be a quantitative measure of CO populations, this analysis shows that the entire ensemble of CO molecules detected by MEIRAS does not exhibit a uniform shift and the fraction of molecules exhibiting an average shift gradually increases with the magnitude of external voltage. Thus, the observed changes in difference spectrum areas are due to a combination of two factors: increasing magnitude of the frequency shift and increasing fraction of molecules exhibiting a shift.

According to previous theoretical analysis of the optical response of the multilayer structure, at small incidence angles with respect to the surface normal, the sensitivity to tangential vibrational modes is significantly larger than the sensitivity to surface normal modes.[37] This means that oblique and horizontally oriented CO molecules are selectively sensed over the normally oriented adsorbed molecules. Thus, a significant fraction of the MEIRAS band at small incidence angles used in this work would likely consist of signal from CO molecules adsorbed on the edges of Pt islands and cracks in the rough Pt film (Figure 7). The contribution to normal mode (corresponding to a larger fraction of CO molecules on top of the Pt film) should

Table 1. Estimation of the Fraction of MEIRAS Band Exhibiting a Shift Equal to the Average Band Center Shift

voltage (V)	average shift in band center (2δ) (cm^{-1})	fractional difference spectrum area of Lorentzian peak (F^{L}_{diff})	measured fractional difference spectrum area (F_{diff})	fraction of band exhibiting the average shift (F_{diff}/F^{L}_{diff})
−2	−1.2	−0.044	−0.043	**0.96**
−1.2	−1.1	−0.040	−0.035	**0.86**
−0.4	−1.1	−0.040	−0.017	**0.43**
0.4	1.9	0.070	0.032	**0.46**
1.2	4.9	0.176	0.115	**0.65**
2	7	0.243	0.155	**0.64**

Table 2. Effect of Infrared Polarization and Incidence Angle on Magnitude of Bias Induced Frequency Shifts in the Catalytic Diode (Black Arrows and Circles Represent Infrared Polarization)

Polarization and incidence angle	s-polarized, 10°	p-polarized, 10°	s-polarized, 50°	p-polarized, 50°
	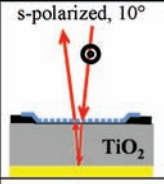	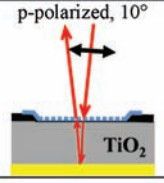	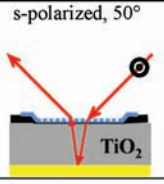	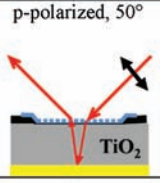
Total area at 0V (A_{total})	4.97 cm^{-1}	5.05 cm^{-1}	6.67 cm^{-1}	4.37 cm^{-1}
Difference spectrum area at -2V (A_{diff})	0.182 cm^{-1}	0.182 cm^{-1}	0.205 cm^{-1}	0.085 cm^{-1}
Fractional area (F_{diff})	**3.7%**	**3.6%**	**3.1%**	**1.9%**

increase with increasing incidence angle of a parallel polarized infrared beam. To investigate the possible effect of orientation of CO molecules being probed, on the magnitude of the frequency shift observed, we performed bias voltage experiments on a catalytic diode as a function of infrared polarization and incidence angle. These experiments were performed by inserting a wire-grid polarizer in the path of the incident infrared beam along with using the variable angle reflection accessory. Incidence angles of 10° and 50° are used with perpendicular (s) and parallel (p) polarizations as shown in Table 2. We calculated the fractional difference spectrum area at a bias voltage of −2 V, for each of the four cases shown in a single experiment with the same ensemble of adsorbed CO molecules. At normal incidence, the s and p polarizations are identical with only a tangential component. Increasing the incidence angle gradually increases the surface normal component of the p-polarized radiation, whereas the s-polarized radiation remains tangential to the surface. In the first three cases considered in Table 2, where only the vibrational modes tangential to the surface are being probed, the magnitude of frequency shift remains about the same. On increasing this normal component, however, the magnitude of fractional difference spectrum area decreases as observed in the case of p-polarized IR radiation at 50° incidence. This analysis indicates that CO molecules oriented tangential to the surface, likely to be adsorbed on the cracks in Pt film in close proximity to Pt/TiO_2 interface, as expected, are more strongly affected by the electron transfer at the interface. This is perhaps one of the first infrared investigations of the effect of molecular orientations on supported catalyst systems since no one, except our group, has used the MEIRAS technique which allows tuning of selectivity to different orientations. These effects are less strongly pronounced in the present versions of our catalytic diode due to surface roughness, but are expected to be more significant in supported model catalysts with a well-defined structure.

The controlled electron transfer from the support to the metal and to adsorbed CO observed here opens the field for the potential manipulation of molecule−surface interactions in catalytic junctions via bias voltages, a hitherto unexplored area of catalysis. Because the system can respond instantly to the external voltage, changing the voltage at frequencies close to the timescales of surface reactions can potentially lead to interesting dynamic phenomena related to surface reactivity. Such transient tuning is not possible in supported ultrathin oxide films or by addition of alkali promoters. The approach presented here can also be used to estimate interfacial electric fields in metal−semiconductor and other diode junctions using the vibrational signature of probe molecules. Thus, the results have potential applications in the areas of sensors, solar, and other electronic devices based on diode junctions. Furthermore, the MEIRAS technique can be used to sense the orientation of adsorbed molecules by changing incidence angle and polarization, as experimentally demonstrated here for the first time. This opens a new area of inquiry into the relation between the surface structure and orientation of molecules adsorbed, regardless of the application of bias voltage.

4. CONCLUSION

The MEIRAS technique combined with a catalytic diode is used to study the Schwab electronic effect of electron transfer using bias voltage as a new variable and without modifying the

dx.doi.org/10.1021/ja2020789 |J. Am. Chem. Soc. 2011, 133, 16459–16467

geometric structure of the catalyst. We provide the first direct demonstration of modification of chemisorption on a supported catalyst by inducing electron transfer through voltage biasing of a metal−support junction. CO is used as a probe molecule on a Pt surface, and the effect of electron transfer in a multilayer catalytic diode is observed as a shift in C−O stretching frequency. The effect of electron transfer is not uniform for all adsorbed molecules and depends on local geometry of catalytic diode near the metal−support interfaces and proximity of adsorbates to these interfaces. The new approach to heterogeneous catalysis developed in this work can potentially provide control of the surface chemical bond by an external voltage, thus, making it an important probe for study of electronic effects that can help the rational design of catalysts. We believe that the catalytic diode is an embryonic concept for the development of selective gas sensing and plasmonic devices, and can be of significant interest to scientists involved in studies of the electronic structure of materials interacting with their environment.

■ ASSOCIATED CONTENT

Supporting Information. Further details on the effect of external voltage on the reflectance of catalytic diode; confirmation of electrical continuity in catalytic diode; calculation of difference spectrum peak area as a function of frequency shifts in fitted Lorentzian peaks. This material is available free of charge via the Internet at http://pubs.acs.org.

■ AUTHOR INFORMATION

Corresponding Author
ewolf@nd.edu

■ ACKNOWLEDGMENT

The support of this work by NSF grant number CBET 08-54324 is gratefully acknowledged.

■ REFERENCES

(1) Somorjai, G. A. *Introduction to Surface Chemistry and Catalysis*; John Wiley & Sons Inc.: New York, 1994.
(2) Tao, F.; Grass, M. E.; Zhang, Y.; Butcher, D. R.; Renzas, J. R.; Liu, Z.; Chung, J. Y.; Mun, B. S.; Salmeron, M.; Somorjai, G. A. *Science* **2008**, *322*, 932–934.
(3) Gunter, P. L. J.; Niemantsverdriet, J. W.; Ribeiro, F. H.; Somorjai, G. A. *Catal. Rev. Sci. Eng.* **1997**, *39*, 77–168.
(4) Campbell, C. T. *Surf. Sci. Rep.* **1997**, *27*, 1–111.
(5) Henry, C. R. *Surf. Sci. Rep.* **1998**, *31*, 231–325.
(6) Boudart, M. *Top. Catal.* **2000**, *13*, 147–149.
(7) Goodman, D. W. *J. Catal.* **2003**, *216*, 213–222.
(8) Freund, H. J. *Chem.—Eur. J.* **2010**, *16*, 9384–9397.
(9) Krauth, A. C.; Bernstein, G. H.; Wolf, E. E. *Catal. Lett.* **1997**, *45*, 177–186.
(10) Krauth, A. C.; Lee, K. H.; Bernstein, G. H.; Wolf, E. E. *Catal. Lett.* **1994**, *27*, 43–51.
(11) Ji, X. Z.; Zuppero, A.; Gidwani, J. M.; Somorjai, G. A. *Nano Lett.* **2005**, *5*, 753–756.
(12) Park, J. Y.; Somorjai, G. A. *Chem. Phys. Chem.* **2006**, *7*, 1409–1413.
(13) Wolf, E. E. Device for treating gases in a microfabricated matrix of catalyst. US Patent 5,688,474, 1997.
(14) Yan, X. M.; Kwon, S.; Contreras, A. M.; Koebel, M. M.; Bokor, J.; Somorjai, G. A. *Catal. Lett.* **2005**, *105*, 127–132.
(15) Gergen, B.; Nienhaus, H.; Weinberg, W. H.; McFarland, E. W. *Science* **2001**, *294*, 2521–2523.
(16) Nienhaus, H.; Bergh, H. S.; Gergen, B.; Majumdar, A.; Weinberg, W. H.; McFarland, E. W. *Phys. Rev. Lett.* **1999**, *82*, 446–449.
(17) Schwab, G. M. *Discuss. Faraday Soc.* **1950**, *8*, 166–171.
(18) Schwab, G. M. *Adv. Catal.* **1978**, *27*, 1–22.
(19) Solymosi, F. *Catal. Rev.* **1968**, *1*, 233–255.
(20) Tauster, S. J.; Fung, S. C.; Garten, R. L. *J. Am. Chem. Soc.* **1978**, *100*, 170–175.
(21) Goodman, D. W. *Catal. Lett.* **2005**, *99*, 1–4.
(22) Sexton, B. A.; Hughes, A. E.; Foger, K. *J. Catal.* **1982**, *77*, 85–93.
(23) Boccuzzi, F.; Chiorino, A.; Manzoli, M.; Lu, P.; Akita, T.; Ichikawa, S.; Haruta, M. *J. Catal.* **2001**, *202*, 256–267.
(24) Soares, J. M. C.; Morrall, P.; Crossley, A.; Harris, P.; Bowker, M. *J. Catal.* **2003**, *219*, 17–24.
(25) Valden, M.; Goodman, D. W. *Science* **1998**, *281*, 1647–1650.
(26) Chen, M.; Goodman, D. W. *Acc. Chem. Res.* **2006**, *39*, 739–746.
(27) Chen, M.; Cai, Y.; Yan, Z. *J. Am. Chem. Soc.* **2006**, *128*, 6341–6346.
(28) Yoon, B.; Häkkinen, H.; Landman, U.; Wörz, A. S.; Antonietti, J. M.; Abbet, S.; Judai, K.; Heiz, U. *Science* **2005**, *307*, 403–407.
(29) Jochum, W.; Eder, D.; Kaltenhauser, G.; Kramer, R. *Top. Catal.* **2007**, *46*, 49–55.
(30) Farmer, J. A.; Campbell, C. T. *Science* **2010**, *329*, 933–936.
(31) Ponec, V. *Stud. Surf. Sci. Catal.* **1982**, *11*, 63–75.
(32) Haller, G. L.; Resasco, D. E. *Adv. Catal.* **1989**, *36*, 173–235.
(33) Hayek, K.; Kramer, R.; Paal, Z. *Appl. Catal., A* **1997**, *162*, 1–15.
(34) Pacchioni, G.; Giordano, L.; Baistrocchi, M. *Phys. Rev. Lett.* **2005**, *94*, 226104.
(35) Ricci, D.; Bongiorno, A.; Pacchioni, G.; Landman, U. *Phys. Rev. Lett.* **2006**, *97*, 36106−1–4.
(36) Grönbeck, H. *J. Phys. Chem. B* **2006**, *110*, 11977–11981.
(37) Hellman, A.; Klacar, S.; Grönbeck, H. *J. Am. Chem. Soc.* **2009**, *131*, 16636–16637.
(38) Zhang, C.; Yoon, B.; Landman, U. *J. Am. Chem. Soc.* **2007**, *129*, 2228–2229.
(39) Sterrer, M.; Risse, T.; Pozzoni, U. M.; Giordano, L.; Heyde, M.; Rust, H. P.; Pacchioni, G.; Freund, H. J. *Phys. Rev. Lett.* **2007**, *98*, 96107:1–4.
(40) Giordano, L.; Pacchioni, G.; Goniakowski, J.; Nilius, N.; Rienks, E. D. L.; Freund, H. J. *Phys. Rev. Lett.* **2008**, *101*, 026102.
(41) Vaida, M. E.; Bernhardt, T. M.; Barth, C.; Esch, F.; Heiz, U.; Landman, U. *Phys. Status Solidi B* **2010**, *247*, 1001–1015.
(42) Sun, Y. N.; Qina, Z. H.; Lewandowskia, M.; Carrascoa, E.; Sterrera, M.; Shaikhutdinov, S.; Freund, H. J. *J. Catal.* **2009**, *266*, 359–368.
(43) Freund, H. J. *Surf. Sci.* **2007**, *601*, 1438–1442.
(44) Sze, S. M.; Ng, K. K. In *Physics of Semiconductor Devices*; John Wiley & Sons, Inc.: Hoboken, NJ, 2007; pp 135−152.
(45) Louhi, J. T. *IEEE Microwave Guided Wave Lett.* **1994**, *4*, 107–108.
(46) Lambert, D. K. *Electrochim. Acta* **1996**, *41*, 623–630.
(47) Deshlahra, P.; Wolf, E. E.; Schneider, W. F. *J. Phys. Chem. A* **2009**, *113*, 4125–4133.
(48) Crowell, J. E.; Crowell, J. E.; Garfunkel, E. L.; Somorjai, G. A. *Surf. Sci.* **1982**, *121*, 303–320.
(49) Campbell, C. T.; Goodman, D. W. *Surf. Sci.* **1982**, *123*, 413–426.
(50) Weaver, M. J.; Zou, S.; Tang, C. *J. Chem. Phys.* **1999**, *111*, 368–381.
(51) Luo, J. S.; Tobin, R. G.; Lambert, D. K. *Chem. Phys. Lett.* **1993**, *204*, 445–450.
(52) Deshlahra, P.; Tiwari, B.; Bernstein, G. H.; Ocola, L. E.; Wolf, E. E. *Surf. Sci.* **2010**, *604*, 79–83.
(53) Deshlahra, P.; Pferfer, K.; Bernstein, G. H.; Wolf, E. E. *Appl. Catal., A* **2011**, *391*, 22–30.
(54) Ozensoy, E.; Min, B. K.; Santra, A. K.; Goodman, D. W. *J. Phys. Chem. B* **2004**, *108*, 4351–4357.

(55) Gao, F.; Wang, Y.; Goodman, D. W. *J. Phys. Chem. C* **2009**, *113*, 14993–15000.
(56) Su, X.; Cremer, P. S.; Shen, Y. R.; Somorjai, G. A. *J. Am. Chem. Soc.* **1997**, *119*, 3994–4000.
(57) Deshlahra, P.; Wolf, E. E. *J. Phys. Chem. C* **2010**, *114*, 16505–16516.
(58) Green, M. A. In *Solar Cells: Operating Principles, Technology, And System Applications*; Prentice-Hall: Englewood Cliffs, NJ, 1982; pp 178−181.
(59) Bjerke, A. E.; Griffiths, P. R.; Theiss, W. *Anal. Chem.* **1999**, *71*, 1967–1974.
(60) Zheng, M. S.; Sun, S. G.; Chen, S. P. *J. Appl. Electrochem.* **2001**, *31*, 749–757.